Operator representation as a new differential optical absorption spectroscopy formalism

Mark Wenig, Bernd Jähne, and Ulrich Platt

UV–visible absorption spectroscopy with extraterrestrial light sources is a widely used technique for the measurement of stratospheric and tropospheric trace gases. We focus on differential optical absorption spectroscopy (DOAS) and present an operator notation as a new formalism to describe the different processes in the atmosphere and the simplifying assumptions that compose the advantage of DOAS. This formalism provides tools to classify and reduce possible error sources of DOAS applications.

OCIS codes: 300.1030, 070.6020, 010.1290, 280.1120.

1. Introduction

A spectral signal on its way from generation in the light source through the atmosphere to the instrument experiences many different transformations. In this paper we introduce a formalism allowing a comparison of those transformations and the corresponding features of differential optical absorption spectroscopy (DOAS).[1] In this comparison we especially aim at the sequencing of the different transformations, each described by an operator, and identify some combination of noncommuting operators that can be assigned to effects such as the I_0 effect or the undersampling problem. Since these effects are based on different instrument and DOAS parameters, the classification of the main error sources can be helpful for the design of new DOAS instruments and to reduce the errors of existing DOAS applications.

2. Differential Optical Absorption Spectroscopy

In this section we describe the DOAS method. The absorption of radiation by matter is described by the Beer–Lambert law. The absorption of light of the intensity $I(\lambda)$ at the wavelength λ as it passes through an absorbing matter $\mathrm{d}l$ is

$$I(\lambda) = I_0(\lambda)\exp\left[-\sigma(\lambda,\ T)\int c(l)\mathrm{d}l\right]. \tag{1}$$

Here $I_0(\lambda)$ is the incident light intensity, $I(\lambda)$ is the transmitted light intensity, $\sigma(\lambda, T)$ is the absorption cross section of the absorbing species that depends on the wavelength and temperature, and $c(l)$ is its concentration. Here the first simplifying assumption is made, namely, the temperature independence of the absorption cross sections. The cross sections can vary with altitude and temperature; therefore excluding it from the integration produces an error. We can reduce this error by using several cross sections for different temperatures, or, if those are linear dependent, by performing *a posteriori* temperature corrections for known temperature profiles. For most applications it is sufficient to use the temperature at the number density maximum of the climatological profile of the corresponding trace gas.[2]

When absorptions are measured in the atmosphere, Eq. (1) has to be applied for the absorption of all trace gases and has to deal with influences of scattering:

$$I(\lambda) = I_0(\lambda)\exp\left[-\sum_i \sigma_i(\lambda)\mathrm{SCD}_i\right]g(\lambda). \tag{2}$$

where the factor $g(\lambda)$ describes additional attenuation by the optical system and by Rayleigh and Mie scattering in the atmosphere and all other broadband structured influences, such as reflection on the ground. The sum in the exponential runs over all

M. Wenig (wenig@gsfc.nasa.gov) is with NASA Goddard Space Flight Center, Greenbelt, Maryland 20771. B. Jähne and U. Platt are with the Institut für Umweltphysik, Heidelberg University, Heidelberg, Germany. B. Jähne is also with the Interdisciplinary Center for Scientific Computing, Heidelberg University, Heidelberg, Germany.

Received 13 February 2004; revised manuscript received 10 September 2004; accepted 17 January 2005.

0003-6935/05/163246-08$15.00/0

trace gases i in the light path l. The slant column density (SCD) is defined as

$$\mathrm{SCD}_i = \int c_i(l)\mathrm{d}l, \tag{3}$$

with c_i being the concentration of the trace gas i and l stands for all possible light paths. The effect of multiple scattering is included in the air-mass factor (AMF) concept that is described in Section 3. The absorption cross sections $\sigma_i(\lambda)$ are well known from measurements in the laboratory and they are characteristic for each trace gas.

Thus far we can transform Eq. (2) into a linear system of equations with respect to SCD_i by taking the logarithm of both sides:

$$\ln I(\lambda) = \ln I_0(\lambda) + \ln g(\lambda) - \sum_i \sigma_i(\lambda)\mathrm{SCD}_i. \tag{4}$$

The basic drawback of Eq. (4) is that neither the initial light intensity $I_0(\lambda)$ nor the attenuation factor $g(\lambda)$ are known exactly, making it impossible to solve for the desired SCD_i. The essential fact that permits the calculation of SCD_i without this knowledge is that these quantities are subject to only low-frequency (LF) variations with respect to λ whereas the absorption cross sections $\sigma_i(\lambda)$ contain both LF and high-frequency (HF) components. They can thus be split into two contributions:

$$\sigma_i = \sigma_i^B + \sigma_i', \tag{5}$$

where σ_i^B and σ_i' are the LF and HF components, respectively.[1,3] If all LF proportions are modeled by a set of appropriate basis functions $\xi_i(\lambda)$,

$$\ln I_0(\lambda) + \ln g(\lambda) - \sum_i \sigma_i^B(\lambda)\mathrm{SCD}_i = \sum_j a_j\xi_j(\lambda), \tag{6}$$

Eq. (4) becomes

$$\ln I(\lambda) = \underbrace{\sum_j a_j\xi_j(\lambda)}_{\mathrm{LF}} - \underbrace{\sum_i \sigma_i'(\lambda)\mathrm{SCD}_i}_{\mathrm{HF}}, \tag{7}$$

which is linear in the unknown quantities a_j and SCD_i and can be solved by a linear least-squares method. The HF part is defined as the differential optical density $D'(\lambda)$ (see Fig. 1). This approach is known as DOAS.

In practice, Eq. (7) has to be modified because the wavelength mapping between the absorption cross sections $\sigma(\lambda)$ and the light intensity measured by the instrument $I(\lambda)$ are not known exactly or can change because of changes in the spectrometer response during use. We can account for the wavelength mapping by introducing an additional shift and squeeze parameter in the argument of the absorption cross section $\sigma'(\lambda)\rightarrow\sigma'(\omega\lambda + \nu)$. This step transforms Eq. (7) from a linear to a nonlinear optimization problem.

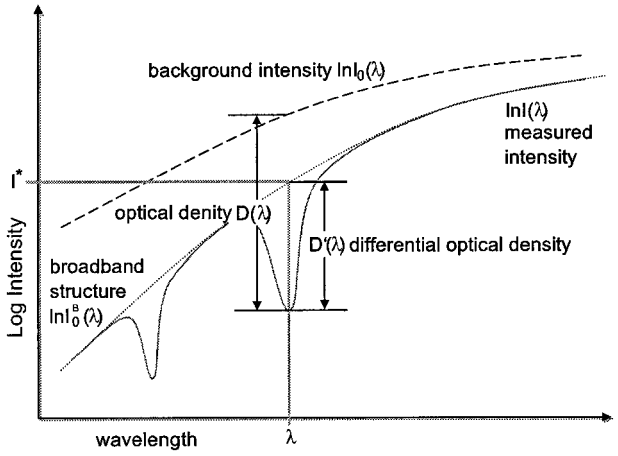

Fig. 1. Correlation of the different parameters used for DOAS.

3. Air-Mass Factor Concept

The resulting SCDs represent the concentration of the specified trace gas integrated over all possible photon paths. Therefore this value is a function of solar zenith angle (SZA) and other parameters such as cloud fraction or ground albedo. To become independent of the viewing geometry, the SCD is transformed into vertical column densities (VCDs). This value represents the concentration integrated along a vertical column through the atmosphere. For this transformation the concept of AMFs[4] has proved to be useful. The AMF is defined as the quotient of SCD and VCD:

$$\mathrm{AMF(SZA)} = \frac{\mathrm{SCD(SZA)}}{\mathrm{VCD}} \Leftrightarrow \mathrm{VCD} = \frac{\mathrm{SCD(SZA)}}{\mathrm{AMF(SZA)}}. \tag{8}$$

Equation (8) suggests that this new value, the VCD, has become independent of the SZA and other measurement conditions, so it can be compared with measurements at different times and locations. However, this is not exactly true as there is a dependence of the AMF on the VCD that causes a nonlinear relation. This nonlinearity, however, can be neglected for weak absorbers, e.g., NO_2. For the calculation of the AMF, knowledge of the SZA, the line of sight, the ground albedo, clouds and aerosols, as well as profile information of all strong absorbing trace gases, mainly O_3, and in particular profile information of the trace gas under investigation is needed. The latter is usually not known and requires *a priori* assumptions or additional measurements or calculations. The AMF can also vary with wavelength. If this variation is small enough, the center of the used wavelength interval can be picked for AMF calculation. For stronger variations of the AMF, selecting the smallest AMF in the DOAS fitting window tends to reduce uncertainties.[2] If the AMF shows a significant wavelength dependence, we can account for this effect by including the wavelength-dependent AMFs in the ab-

sorption cross section. This modified DOAS version allows for the direct fitting of VCDs. We can perform the calculation of the AMF, for example, by solving the radiative transfer equation numerically or by simulating the extinction events in the atmosphere using a Monte Carlo model. This part of a DOAS evaluation is often the largest error source.

4. Differential Optical Absorption Spectroscopy Operator Formalism

In the following, an operator concept is used to describe the DOAS evaluation process. We use the well-known operator definition as functions that map a function on another function, so they can be used to describe the change in the spectrum $f(\lambda)$ on the way through the atmosphere and the detector.

When using the Beer–Lambert law and the already introduced variables to model the extinctions in the atmosphere, we can write the measured spectrum as

$$I(\lambda) = I_0(\lambda) g(\lambda) \exp\left[-\sum_i \sigma_i'(\omega_i \lambda + \nu_i) \mathrm{SCD}_i\right], \quad (9)$$

where ν and ω are shift and squeeze parameters. However, there are still some operations missing that also modify the signal. The spectrum is convoluted with the aperture function (see below) and is discretized. This entails the need for an interpolation algorithm. To obtain a better overview, an operator notation is used to describe all these manipulations of the signal. In the following, $f(\lambda)$ stands for a general function, or spectra in this case.

- Discretizing operator:

$$\mathcal{D}(m,\ b) f(\lambda) = \sum_i \delta(mi + b) f(\lambda). \quad (10)$$

This operator maps a continuous signal on discrete lattice points (pixels) and is realized by a multiplication with a Dirac delta comb.[5] These equidistant points are given by $mi + b$ where m is the difference between the center wavelengths, b is the wavelength offset, and i is the pixel number. These two parameters are considered to stay constant, so they do not have to be fitted in the DOAS optimization.

- Instrument's optical function:

$$\mathcal{A} f(\lambda) = a(\lambda) * f(\lambda) = \int_{-\infty}^{\infty} a(\lambda - \lambda') f(\lambda') \mathrm{d}\lambda'. \quad (11)$$

This operator describes the characteristics of the spectrometer. This is influenced by the instrument's slit function, the properties of a predisperser prism if present and other optical devices, and the sensitivity of the photodiodes. This operator has no parameter that has to be fitted.

- Wavelength registration (shift $\mathcal{S}_h$ and squeeze $\mathcal{S}_q$):

$$\mathcal{S}_h(\nu) f(\lambda) = f(\lambda + \nu), \quad (12)$$

$$\mathcal{S}_q(\omega) f(\lambda) = f(\omega \lambda), \quad (13)$$

$$\mathcal{S} f(\lambda) = \mathcal{S}_h \mathcal{S}_q f(\lambda) = f(\omega \lambda + \nu). \quad (14)$$

This operator should compensate possible changes or errors in the wavelength calibration. The two parameters ν (shift) and ω (squeeze) are nonlinear fitting parameters with respect to $f(\lambda)$. This operator can also include calibration corrections of higher order if needed.

- High- and low-pass filter:

$$\mathcal{T}(n) f(\lambda) = P^n(\lambda), \quad (15)$$

$$\mathcal{H}(n) f(\lambda) = (1 - \mathcal{T}) f(\lambda) = f(\lambda) - P^n(\lambda). \quad (16)$$

These are bandpass filters. Frequently a polynomial $p^n(\lambda) = \sum_0^n p_k \lambda^k$ is used to model the broadband structure. These $(n + 1)$ parameters $(p_0 \ldots p_n)$ are linear fitting parameters.

- Interpolation:

$$\mathcal{B} f(\lambda) = b(\lambda) * f(\lambda) = \int b(\lambda - \lambda') f(\lambda') \mathrm{d}\lambda'. \quad (17)$$

This interpolation is necessary to transform a spectrum from a discrete representation (e.g., after application of the discretization operator $\mathcal{D}$) to a continuous spectrum. This is a nontrivial task when there is a shift and squeeze operator involved; see also Subsection 5.C.

- Logarithm and exponential function:

$$\mathcal{E} f(\lambda) = \exp[f(\lambda)], \quad (18)$$

$$\mathcal{L} f(\lambda) = \mathcal{E}^{-1} f(\lambda) = \ln f(\lambda). \quad (19)$$

These functions are written in this notation to provide a coherent description.

- Scale operator:

$$\mathcal{S}_c(a) f(\lambda) = a f(\lambda). \quad (20)$$

This is a scaling of the function and gives one linear fitting parameter. This operator can be replaced if a nonlinear scaling is needed, e.g., if saturation effects must be considered.

For further simplification, the scaling and the summation of the different absorption cross sections are defined as

$$\tau(\lambda) = -\sum_i \mathcal{S}_c(S_i) \sigma_i'(\lambda) = -\sum_i S_i \sigma_i'(\lambda), \quad (21)$$

and the scaled sum of the solar spectrum I_0 and the Ring spectrum R is named

$$I_S = \mathcal{S}_c(S_{I0})I_0(\lambda) + \mathcal{S}_c(S_R)R(\lambda), \quad (22)$$

where S_{I_o} and S_R are the fitting parameter of the Fraunhofer and Ring spectra.

Using the introduced notation we can formulate the measurement process as follows:

$$I(\lambda) = \mathcal{D}(m,\ b)\mathcal{A}\mathcal{S}(\nu,\ \omega)g(\lambda)I_S\mathcal{E}\tau(\lambda). \quad (23)$$

Because all described operators, except $\mathcal{L}$ and $\mathcal{E}$, are linear, they commutate with the scale operator and can be exchanged with the summation. Therefore all the following considerations refer to all trace gases represented by $\tau(\lambda)$. Also, for simplification the same shift and squeeze operator is used for all trace gas reference spectra.

In the following, the transformation of the modeled spectrum on the path of the radiation through the atmosphere and the instrument is described (see Fig. 2). After passing the atmosphere and being influenced by the different extinction processes, the incoming light is described by $g(\lambda)I_S\mathcal{E}\tau(\lambda)$. As $\tau(\lambda)$ includes reference cross sections, a possibly wrong wavelength calibration has to be corrected by the shift and squeeze operator $\mathcal{S}(\nu, \omega)$ [see Eq. (14)]. Then the signal experiences the influence of the instrument's optics described by the operator $\mathcal{A}$ [see Eq. (11)]. Subsequently the continuous signal is sampled on the detector array described by the operator $\mathcal{D}(m, b)$ where m and b are intrinsic parameters of the instrument and do not need to be considered in the following formulas. However, this is not exactly the function that is used for the fitting process with DOAS. The considerations described in Section 2 are now repeated with this new notation, describing the actual DOAS measurement and evaluation process, this time including convolution and sampling.

First the logarithm operator is applied on both sides of Eq. (23):

$$\begin{aligned}\mathcal{L}I(\lambda) &= \mathcal{L}\{\mathcal{D}\mathcal{A}\mathcal{S}[g(\lambda)I_S\mathcal{E}\tau(\lambda)]\} \\ &= \mathcal{L}\mathcal{D}\mathcal{A}\mathcal{S}g(\lambda) + \mathcal{L}\mathcal{D}\mathcal{A}\mathcal{S}I_S\mathcal{E}\tau(\lambda). \end{aligned} \quad (24)$$

In the next step in a typical DOAS evaluation, the relation $\mathcal{L}\mathcal{E} = \mathbf{1} =$ unity operator is used. This can be exploited only when either $\mathcal{L}$ or $\mathcal{E}$ commutes with the operators $\mathcal{D}$, $\mathcal{A}$, and $\mathcal{S}$. With the usual definition (Poisson brackets) $[A, B] = AB - BA$, this means

$$[\mathcal{L},\ \mathcal{D}] = 0,\ \ [\mathcal{L},\ \mathcal{A}] = 0,\ \ [\mathcal{L},\ \mathcal{S}] = 0, \quad (25)$$

or

$$[\mathcal{E},\ \mathcal{D}] = 0,\ \ [\mathcal{E},\ \mathcal{A}] = 0,\ \ [\mathcal{E},\ \mathcal{S}] = 0. \quad (26)$$

This can be easily shown to hold for $\mathcal{D}$ and $\mathcal{S}$. However, the commutator of $\mathcal{L}$ and $\mathcal{A}$, and therefore also the commutator of $\mathcal{E}$ and $\mathcal{A}$, does not vanish in general. Nevertheless this effect is neglected here for further calculations. As $\mathcal{L}\mathcal{A}$ is applied on $I_S\mathcal{E}\tau$ it can also be commuted by means of neglecting the commutator $\mathcal{L}[\mathcal{E}\tau, \mathcal{A}I_S]$, which of course is also not zero. This effect is called the I_0 effect[6] and is described in Subsection 5.A. It can be shown that it is possible to correct the cross sections f in a way that the influence of this commutator is reduced, which is called the I_0 correction.[6] Thus Eq. (24) becomes

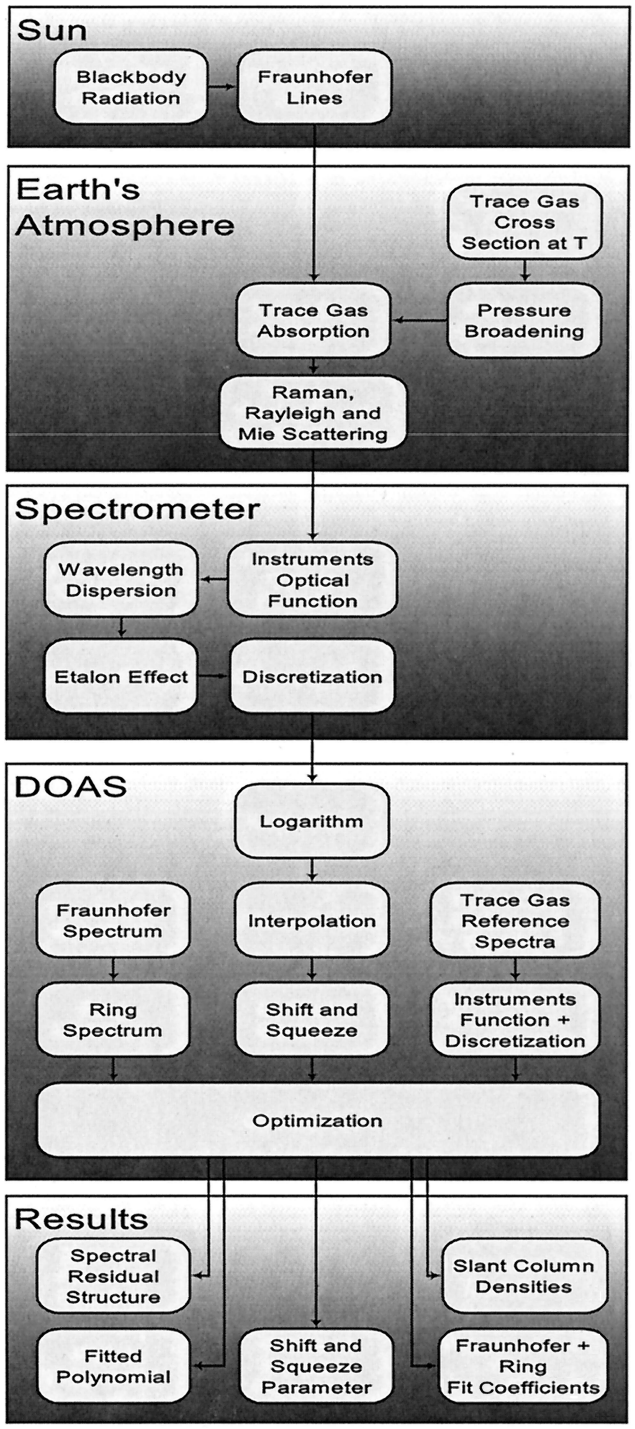

Fig. 2. Overview of the formation of the signal, the processes in the atmosphere, the influences of the measurement on the signal, and the DOAS optimization process.

$$\mathcal{L}I(\lambda) = \mathcal{L}\mathcal{D}\mathcal{A}\mathcal{S}g(\lambda) + \mathcal{D}\mathcal{L}\mathcal{A}\mathcal{S}\mathcal{I}_S + \mathcal{D}\mathcal{A}\mathcal{S}\mathcal{L}\mathcal{E}\tau(\lambda) = \mathcal{L}\mathcal{D}\mathcal{A}\mathcal{S}g(\lambda) + \mathcal{D}\mathcal{L}\mathcal{A}\mathcal{S}\mathcal{I}_S + \mathcal{D}\mathcal{A}\mathcal{S}\tau(\lambda). \quad (27)$$

As we are interested in the HF part of the spectrum, we add a unity operator written in the form $\mathbf{1} = \mathcal{T} + \mathcal{H}$ that separates the signal into the HF and LF part:

$$\begin{aligned}\mathcal{L}I(\lambda) &= (\mathcal{T} + \mathcal{H})\mathcal{L}\mathcal{D}\mathcal{A}\mathcal{S}g(\lambda) + (\mathcal{T} + \mathcal{H})(\mathcal{D}\mathcal{L}\mathcal{A}\mathcal{S}\mathcal{I}_S(\lambda) \\ &\quad + (\mathcal{T} + \mathcal{H})\mathcal{D}\mathcal{A}\mathcal{S}\tau(\lambda) \\ &= \mathcal{T}[\mathcal{L}\mathcal{D}\mathcal{A}\mathcal{S}g(\lambda) + \mathcal{D}\mathcal{A}\mathcal{S}\tau(\lambda) + \mathcal{D}\mathcal{L}\mathcal{A}\mathcal{S}\mathcal{I}_S(\lambda)] \\ &\quad + \mathcal{H}\mathcal{L}\mathcal{D}\mathcal{A}\mathcal{S}g(\lambda) + \mathcal{H}\mathcal{D}\mathcal{L}\mathcal{A}\mathcal{S}\mathcal{I}_S(\lambda) + \mathcal{H}\mathcal{D}\mathcal{A}\mathcal{S}\tau(\lambda).\end{aligned} \quad (28)$$

Now we make an assumption that the initial intensity and the influence of scattering, expressed by $g(\lambda)$, is fully represented by broadband structures, i.e., the term $\mathcal{H}\mathcal{L}\mathcal{D}\mathcal{A}\mathcal{S}g(\lambda)$ can be neglected. This is the main principle of DOAS. The advantage of using the low-pass filter $\mathcal{T}$ is that only $n + 1$ linear polynomial coefficients have to be fitted and it is not necessary to model g, the LF part of I_S, or the associated shift and squeeze parameter.

This is still not the form we can use for the fitting process as the reference spectra are not all known as a continuous high-resolved function, especially the solar reference that is usually measured with the spectrometer itself and is therefore influenced by the aperture function and the sampling. So we need the term $\mathcal{D}\mathcal{A}I_S(\lambda)$ and $\mathcal{D}\mathcal{A}\tau(\lambda)$ in the formula. This can be achieved when we add the commutator of $\mathcal{S}$ and $\mathcal{A}$, but it has to be investigated if this commutator vanishes. As it does not, this analysis is described in Subsection 5.B. Now we obtain

$$\mathcal{L}I(\lambda) = T[\ldots] + \mathcal{H}\mathcal{D}\mathcal{S}\mathcal{L}\mathcal{A}I_S(\lambda) + \mathcal{H}\mathcal{D}\mathcal{S}\mathcal{A}\tau(\lambda). \quad (29)$$

The next comutator would be $[\mathcal{D},\mathcal{S}]$, but this one does not vanish because the right-hand side of $\mathcal{S}$ must be a continuous function, so $\mathcal{S}\mathcal{D}\tau(\lambda)$ would make no sense. When the shift and squeeze operator should be applied to a discrete function, this function has to be interpolated for intermediate grid points first. This can be done by use of the interpolation operator $\mathcal{B}$. So we insert $\mathcal{B}\mathcal{D}$ in the formula:

$$\begin{aligned}\mathcal{L}I(\lambda) &= \mathcal{T}[\ldots] + \mathcal{H}\mathcal{D}\mathcal{S}\mathcal{B}\mathcal{D}\mathcal{L}\mathcal{A}I_S(\lambda) + \mathcal{H}\mathcal{D}\mathcal{S}\mathcal{B}\mathcal{D}\mathcal{A}\tau(\lambda) \\ &= \mathcal{T}[\ldots] + \mathcal{H}\mathcal{D}\mathcal{S}\mathcal{B}\mathcal{L}\mathcal{D}\mathcal{A}I_S(\lambda) + \mathcal{H}\mathcal{D}\mathcal{S}\mathcal{B}\mathcal{D}\mathcal{A}\tau(\lambda).\end{aligned} \quad (30)$$

Again this operation causes an uncertainty that is called the undersampling effect. If the sampling frequency of $\mathcal{D}$ is below the Nyquist frequency, the signal cannot be fully reconstructed. The influence of this effect is described in Subsection 5.C.

In most implementations the high-pass filtering $\mathcal{H}$ is also neglected, which does not influence the fit result because this means only a change in the fitted polynomial. In addition, $\ln(I_S) = \ln[S_{I_o}I_0(\lambda) + S_RR(\lambda)]$ is replaced by $S_{I_o}\ln[I_0(\lambda)] + S_RR(\lambda)/I_0(\lambda)$, which is an approximation that preserves linearity for the fitting coefficients. So finally we obtain

$$\begin{aligned}\mathcal{L}I(\lambda) &= \mathcal{T}(n_0, n_1, n_2, n_3)[\ldots] \\ &\quad + \mathcal{S}_c(S_{I_o})\mathcal{S}(\nu_0, \omega_0)\mathcal{B}\mathcal{L}\mathcal{D}\mathcal{A}I_0'(\lambda) \\ &\quad + \mathcal{S}_c(S_R)\mathcal{S}(\nu_1, \omega_1)\mathcal{B}\mathcal{L}\mathcal{R}(\lambda) \\ &\quad - \sum_i \mathcal{D}\mathcal{S}(\nu_1, \omega_1)\mathcal{B}\mathcal{D}\mathcal{A}\mathcal{S}_c(S_i)\sigma_i'(\lambda),\end{aligned} \quad (31)$$

with the linear fitting parameters $n_0, n_1, n_2, n_3, S_i, S_{I_o}$, S_R and the nonlinear ν_i, ω_i.

5. Sample Applications of the Operator Concept

Now the above described operator notation is exploited to describe accompanying errors when we apply DOAS. Most of the resulting errors arise from the fact that DOAS assumes a different sequence of transformations of the spectrum than actually occur.

As an application sample we used a DOAS evaluation of data from the Global Ozone Monitoring Experiment[7] (GOME) aboard the European Space Agency's second European Remote Sensing Satellite (ERS-2). In this case solar radiation scattered from the atmosphere or reflected from the ground is analyzed by the observing instrument.

A. I_0 Effect

Because of the large number of Fraunhofer lines, the intensity of the solar spectrum varies strongly with wavelength, as do the strong absorbers in the terrestrial atmosphere. Thus the approximations that lead to Eq. (31) are not fulfilled. In particular, for trace gases also showing narrow spectral structures, the absorptions found in measured atmospheric spectra cannot be fitted properly by the respective cross sections (which are usually measured in the laboratory by a light source with a smooth spectrum, e.g., a blackbody radiator). Because these errors arise from the spectral structures of the I_0 spectrum, it is usually referred to as the solar I_0 effect.[6,8,9]

This effect can be described by the nonvanishing commutator $[\mathcal{E}(-\sigma\mathrm{SCD}), \mathcal{A}I_0]$. The question is, under which conditions can this effect be neglected? To answer this question, the following calculation can be made:

$$\begin{aligned}&[\mathcal{E}(-\sigma_{I0}\mathrm{SCD}),\ \mathcal{A}I_0](\lambda) = 0, \\ &\Leftrightarrow \mathcal{E}[-\sigma_{I0}(\lambda)\mathrm{SCD}]\mathcal{A}I_0(\lambda) - \mathcal{A}I_0(\lambda)\mathcal{E}[-\sigma_{I0}(\lambda)\mathrm{SCD}] = 0, \\ &\Leftrightarrow -\sigma_{I0}(\lambda)\mathrm{SCD} = \mathcal{L}\mathcal{A}I_0(\lambda)\mathcal{E}[-\sigma_{I0}(\lambda)\mathrm{SCD}] - \mathcal{L}\mathcal{A}I_0(\lambda), \\ &\Leftrightarrow \sigma_{I0}(\lambda) = -\frac{1}{\mathrm{SCD}}\ln\frac{\mathcal{A}\{I_0\exp[-\sigma_{I0}(\lambda)\mathrm{SCD}]\}}{\mathcal{A}I_0}.\end{aligned} \quad (32)$$

The last line gives an equation for the combination of absorption cross sections and the solar I_0 spectrum for which the solar I_0 effect can be neglected. The I_0 effect has to be considered in the case when strong Fraun-

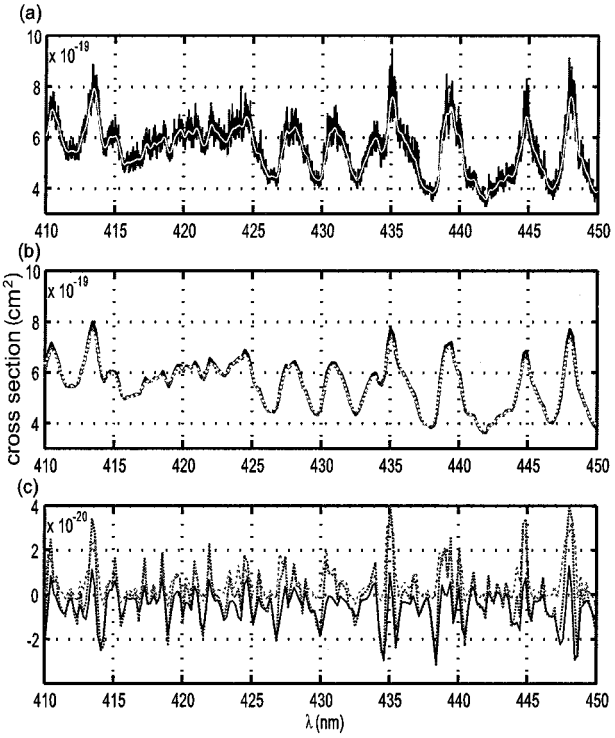

Fig. 3. Influence of the I_0 effect on the reference spectrum of NO_2. (a) The high-resolved original spectrum (dark curve) and the I_0-corrected spectrum in (light curve). (b) The original (solid curve), the I_0-corrected spectrum (dashed curve), and the smoothed signal (dotted curve) in GOME resolution ($\mathcal{D}\mathcal{A}$ applied). (c) Deviation of the I_0-corrected (dashed curve) and the smoothed (dotted curve) spectrum to the original spectrum and the difference between the I_0-corrected and the smoothed spectrum (solid curve) (from Beirle[11]).

hofer lines or atmospheric absorbers like O_3 have to be removed to measure the underlying weak absorptions of other trace gases. The solar I_0 effect (i.e., the I_0 effect due to Fraunhofer lines) can be accounted for by use of the so-called I_0-corrected cross sections.

This correction was first introduced by Johnston.[10] We can obtain the corrected cross section by applying the commutation:

$$\mathcal{C}[-\sigma_{\text{corr}}(\lambda)\text{SCD}]\mathcal{A}I_0(\lambda) = \mathcal{A}I_0(\lambda)\mathcal{C}[-\sigma_{\text{orig}}(\lambda)\text{SCD}]$$
$$\Leftrightarrow \sigma_{\text{corr}}(\lambda) = -\frac{1}{\text{SCD}}\ln\frac{\mathcal{A}\{I_0\exp[-\sigma_{\text{orig}}(\lambda)\text{SCD}]\}}{\mathcal{A}I_0}. \quad (33)$$

Of course the SCD of the trace gas is unknown; however, we can iterate Eqs. (33) by first determining SCD_0 from an evaluation without I_0 correction and then apply the new fitted SCD using the corrected cross section till the cross sections converge. It should be mentioned that the commutator is applied to the sum of cross sections since normally more than one trace species is fitted and therefore the I_0 correction would have to be done simultaneously, which is not possible because Eqs. (32) are not linear in σ.

In Fig. 3 the influence of the I_0-corrected effect on the original NO_2 reference spectrum is shown. As Eqs. (32) are similar to a normalized convolution, the correction is similar to a smoothing of the spectrum. For the GOME DOAS analysis, for example, this effect can be suppressed by means of smoothing the spectra in advance.

B. Commutator of Shift and Squeeze and Folding

As mentioned in Section 4, when we apply the DOAS technique, the commutator of the shift and squeeze operator $\mathcal{S}$ and the convolution with the instrument function $\mathcal{A}$ are neglected. As $\mathcal{A}$ is by definition a shift-invariant filter, only the commutator $[\mathcal{S}_c, \mathcal{A}]$ has to be analyzed.

Within the scope of most DOAS applications the squeeze parameter ω can be assumed to be close to unity: $\omega = 1 + \epsilon$ with $\epsilon \ll 1$ (in practice only $\epsilon < 0.01$ occurs).

We start with the operation $\mathcal{S}_c(\omega)\mathcal{A}$:

$$\mathcal{S}_c(\omega)\mathcal{A}f(x) = (h * f)(\omega x)$$
$$= \int h(\omega x - x')f(x')\mathrm{d}x'$$
$$= \omega\int h[\omega(x-\xi)]f(\omega\xi)\mathrm{d}\xi, \quad (34)$$

where $h(x)$ is the convolution kernel of $\mathcal{A}$. Now the term $h[\omega(x-\xi)]$ can be expanded in a Taylor series in ω around one.[12] Because $\omega \approx 1$, the series can be cut after the term of order one assuming a sufficient smooth function h. Then Eq. (34) becomes

$$\mathcal{S}_c(\omega)\mathcal{A}f(x) \approx \omega\int [h(x-\xi) + (\omega-1)$$
$$\times (x-\xi)h'(x-\xi)]f(\omega\xi)\mathrm{d}\xi$$
$$= \omega h(x) * f(\omega x) + \omega(\omega-1)$$
$$\times \int (x-\xi)h'(x-\xi)f(\omega\xi)\mathrm{d}\xi$$
$$\approx \omega h(x) * f(\omega x) + \epsilon\int (x-\xi)h'$$
$$\times (x-\xi)f(\omega\xi)\mathrm{d}\xi. \quad (35)$$

Approximation (35) shows that the introduced error coming from the commutation of $\mathcal{A}$ and $\mathcal{S}_c$ is dominated by convolution of the squeezed signal with a new kernel $xh'(x)$. To analyze this more closely, the filter kernel $h(x)$ is replaced by a Gauss function $h(x) \approx \mathcal{G}_\sigma \equiv 1/\sqrt{2\pi}\sigma\exp[-1/2(x/\sigma)^2]$. Then we can calculate the first and second derivative:

$$\frac{\mathrm{d}}{\mathrm{d}x}h(x) = -\frac{x}{\sigma^2}h(x), \quad (36)$$

$$\frac{\mathrm{d}^2}{\mathrm{d}x^2}h(x) = \left(\frac{x^2}{\sigma^4} - \frac{1}{\sigma^2}\right)h(x). \quad (37)$$

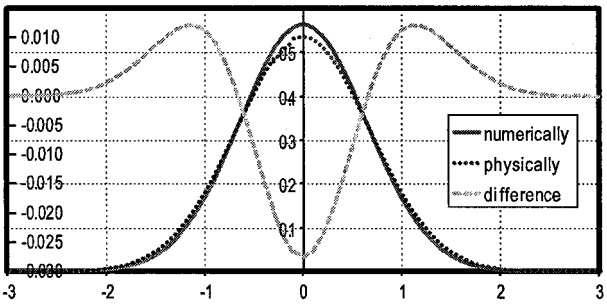

Fig. 4. Resulting error curve after $[\mathcal{S}_c, \mathcal{A}]$ is applied to a Gaussian signal [see Eq. (39)]. The instrument's optical function was also modeled by a Gaussian function with $\sigma_h = 0.5$, and the squeeze parameter was chosen as $\omega = 1.1$, which is exaggerated to emphasize this effect. The physically correct operation $\mathcal{A}\mathcal{S}(0.0, 1.1)$ is shown as a dotted curve; the numerically used operation $\mathcal{S}(0.0, 1.1)\mathcal{A}$ is shown as a solid curve. The dashed curve shows the difference between these two curves $[\mathcal{S}_c, \mathcal{A}]$ (left scale).[12]

Accordingly the new filter kernel $xh'(x)$ can be written as

$$xh'(x) = -\frac{x}{\sigma^2} h(x)x,$$

$$= -\sigma^2 h''(x) - h(x). \tag{38}$$

Combining Eqs. (35) and (38) results in

$$(h * f)(\omega x) \approx \omega h(x) * f(\omega x) - \epsilon h(x) * f(\omega x) - \epsilon\sigma^2 \int h''(x - \xi) f(\omega\xi) d\xi$$

$$= h(x) * f(\omega x) - \epsilon\sigma^2 \int h''(x - \xi) f(\omega\xi) d\xi$$

$$= h(x) * f(\omega x) - \epsilon\sigma^2 \int h(x - \xi)\omega^2 f''(\omega\xi) d\xi$$

$$\approx h(x) * f(\omega x) - \epsilon\sigma^2 h(x) * f''(\omega x)$$

$$= \mathcal{S}_c(\omega)\mathcal{A}\mathcal{S}_c(\omega) f(x) - \epsilon\sigma^2 \int h(x - \xi)\omega^2 f''(\omega\xi) d\xi$$

$$\approx h(x) * f(\omega x) - \epsilon\sigma^2 h(x) * f''(\omega x),$$

$$\Rightarrow [\mathcal{S}_c, \mathcal{A}] f(x) \approx \epsilon\sigma^2 h(x) * f''(\omega x). \tag{39}$$

Therefore the error introduced by the commutation of folding and squeezing is proportional to the second derivative of the squeezed signal folded with the instrument's optical function. For the case of a highly localized signal, e.g., emission or absorption bands, the effect is shown in Fig. 4. It can be observed that the function that is used for DOAS underestimates the physically correct line in the full width at half-maximum (FWHM), which leads to an overestimation of the fitted slant column density and a contribution to the residuum with roughly twice the frequency of the reference spectrum.

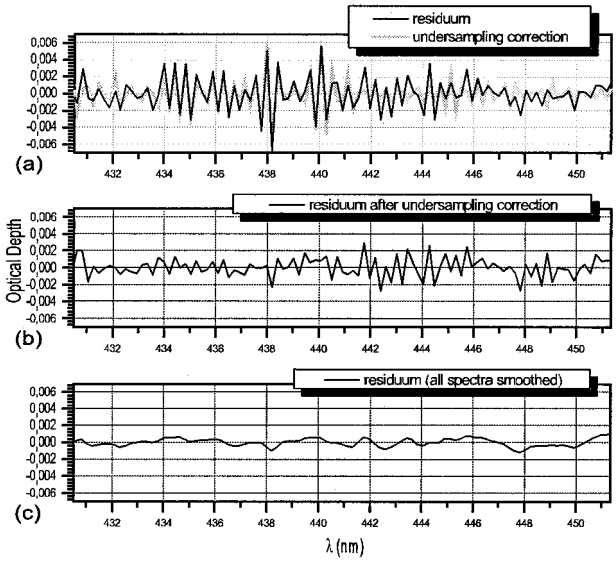

Fig. 5. Demonstration of the undersampling effect. (a) Residuum of a NO_2 fit of GOME spectrum 775 from 20 August 1997 and the calculated undersampling correction $\mathcal{D}\mathcal{S}\mathcal{R}\mathcal{D}\mathcal{A}I_0 - \mathcal{D}\mathcal{S}\mathcal{A}I_0$. The χ^2 is 4.3×10^{-4}, and the fitted NO_2 absorption of this fit is $(-3.86 \times 2.45)10^{15}$ with a shift of 0.0070 nm. (b) The reduced residuum after the undersampling correction is applied. The χ^2 reduces to 1.4×10^{-4}, and the NO_2 absorption slightly changed to $(-3.84 \times 1.41)10^{15}$ with a shift of 0.0060 nm. (c) Fit result of the same spectrum without the described undersampling correction but with smoothed spectra (from Beirle[11]).

The intensity of this effect is proportional to σ^2, which means that it is stronger for less localized instrument functions. The ideal instrument function is a δ function and this effect vanishes. For example, the GOME instrument σ is around 1.5; and as typical values for ϵ are around 1%, the described influence can be neglected for the DOAS calculation and can be included in the subsequent error analysis. The influences of the described effect can be further suppressed by means of smoothing the incoming signal beforehand.

C. Spectral Undersampling

In Eq. (30) the operator $\mathcal{D}\mathcal{S}\mathcal{R}\mathcal{D}\mathcal{A} - \mathcal{D}\mathcal{S}\mathcal{A}$ was applied to take into account that the measured solar reference spectrum is available only on a discrete wavelength grid. A spectrum can be reconstructed only when the sampling condition of the Nyquist theorem is met. This is not always the case (e.g., for the GOME instrument because the solar spectrum has structures with much higher frequencies than GOME can measure). Since the interpolation reproduces the signal at the grid points, this undersampling effect appears only when there is a shift or squeeze of the wavelength mapping involved while different measured spectra are com-

pared. The undersampling effect can be analyzed with the operator $\mathcal{DSBDA} - \mathcal{DSA}$ applied to a high-resolved solar spectrum. The results can be seen in Fig. 5. It can be observed that the result of this calculation is similar to the residuum of the DOAS fit. With this spectrum used as an additional cross section, the new residuum can be reduced. However, the effect on the NO_2 fit result is small. The χ^2 reduces from 4.3×10^{-4} to 1.4×10^{-4} whereas the NO_2 VCD changes only from $(-3.86 \pm 2.45)10^{15}$ molecules/cm^2 to $(-3.84 \pm 1.41)10^{15}$ molecules/cm^2. A reduction of the NO_2 error in the same order of magnitude can be achieved by a preceding smoothing of the references, which can be expressed when $\mathcal{H}$ is replaced by $\mathcal{G}$ in Eq. (28), where $\mathcal{G}$ is a bandpass filter that damps LFs and HFs. This frequency clipping can also be achieved by use of a less localized instruments function.

Since the operator $\mathcal{DSBDA} - \mathcal{DSA}$ can be used to measure the undersampling effect separately from other error sources, it is a helpful tool for the design of new instruments.

6. Conclusion

The DOAS formalism described in this paper is a new way to describe the basic assumptions that are necessary for a DOAS measurement. These are simplifying assumptions about the influence of extinction processes in the atmosphere and the measuring process on the spectral signal. Furthermore this formalism allows one to differentiate possible error sources of the DOAS method and provides tools to reduce these errors. Use of operators to describe a DOAS measurement leads directly to the well-known I_0 effect, allows one to separate and visualize the undersampling effect, and also allows one to discover the effect of the nonvanishing commutator of squeezing and folding.

References

1. J. Stutz and U. Platt, "Numerical analysis and error estimation of differential optical absorption spectroscopy measurements with least-squares methods," Appl. Opt. **35,** 6041–6053 (1996).
2. J. Burrows, M. Weber, M. Buchwitz, V. Rozanov, A. Ladstaetter-Weissenmayer, A. Richter, R. Debeek, R. Hoogen, K. Bramstedt, K.-U. Eichmann, M. Eisinger, and D. Perner, "The Global Ozone Monitoring Experiment (GOME): mission concept and first results," J. Atmos. Sci. **56,** 151–175 (1999).
3. U. Platt, "Differential optical absorption spectroscopy (DOAS)," in *Air Monitoring by Spectrometric Techniques,* Vol. 127 of Chemical Analysis Series, M. W. Sigrist, ed. (Wiley, New York, 1994), pp. 27–84.
4. L. M. Perliski and S. Solomon, "On the evaluation of air mass factors for atmospheric near-ultraviolet and visible absorbers," J. Geophys. Res. **98,** 10363–10374 (1993).
5. B. Jähne, *Handbook on Computer Vision and Applications,* (Academic, San Diego, Calif., 1999), Vol. 2, Chap. 8, pp. 179–196.
6. S. R. Aliwell, M. Van Roozendael, P. V. Johnston, A. Richter, T. Wagner, D. W. Arlander, J. P. Burrows, D. J. Fish, R. L. Jones, K. K. Trnkvist, J.-C. Lambert, K. Pfeilsticker, and I. Pundt, "Analysis for BrO in zenith-sky spectra: an intercomparison exercise for analysis improvement," J. Geophys. Res. **107D,** 10.1029/2001/JD000329 (2002).
7. F. Bednarz, *Global Ozone Monitoring Experiment, GOME, Users Manual* (European Space Agency, Noordwijk, The Netherlands, 1995).
8. U. Platt, L. Marquard, T. Wagner, and D. Perner, "Corrections for zenith scattered light DOAS," Geophys. Res. Lett. **24,** 1795–1762 (1997).
9. A. Richter, Absorptionsspektroskopische Messungen stratosphärischer Spurengase über Bremen, 53°," Ph.D. dissertation (Universität Bremen, Bremen, Germany, 1997).
10. P. Johnston, National Institute of Water and Atmospheric Research, Auckland, New Zealand (personal communication, 2004).
11. S. Beirle, Institute of Environmental Physics, Heidelberg, Germany (personal communication, 2001).
12. C. Leue, "Detektion der troposphärischen NO_2 Daten anhand von GOME," Ph.D. dissertation (University of Heidelberg, Heidelberg, Germany, 1999).